Available online at www.sciencedirect.com
SCIENCE DIRECT®
Chemometrics and Intelligent Laboratory Systems 83 (2006) 26–33
Chemometrics and intelligent laboratory systems
www.elsevier.com/locate/chemolab

Identification of long-range aerosol transport patterns to Toronto via classification of back trajectories by cluster analysis and neural network techniques

Sandy Owega, Badi-Uz-Zaman Khan, Greg J. Evans *, Robert E. Jervis, Mike Fila

Department of Chemical Engineering and Applied Chemistry, University of Toronto, 200 College Street, Toronto, Ontario, Canada, M5S 3E5

Received 18 March 2004; received in revised form 19 December 2005; accepted 20 December 2005
Available online 28 February 2006

Abstract

In this work, back trajectories of air masses arriving in Toronto were classified into distinct transport patterns by cluster analysis and, for the first time, by a neural network (Adaptive Resonance Theory—ART-2a). Different similarity criteria were used by the two classification techniques, the former relying on the Euclidean distances between trajectories, the latter on the Euclidean angles between trajectories. Nevertheless, both techniques provided similar conclusions as to the location of $PM_{2.5}$ emission sources and the level of pollution associated with a given air transport pattern. Both techniques illustrated the cleaner nature of northerly and northwesterly transport patterns in comparison to southerly and southwesterly ones, as well as the effect of near stagnant air masses. In addition, ART-2a resolved a much larger percentage of trajectories than cluster analysis into groups with clearly identifiable transport patterns and compared favourably with cluster analysis with respect to the precision of the classification.

Keywords: Air pollution; Atmospheric aerosol; Fine particulate matter; Long-distance transport; Ontario

1. Introduction

Identifying the sources of airborne pollutants is of great importance to the study of fine particulate matter ($PM_{2.5}$), which has been linked to adverse health effects [1]. The examination of transport patterns of air masses through the use of back trajectories is commonly performed for source identification. Unlike wind direction, back trajectories provide visualization of not just the local air direction, but transport over a continental scale. While back trajectories are on average accurate to within 20% of the distance traveled, individual back trajectories may be completely incorrect [2]. Thus, a large dataset is required to provide meaningful source identification.

Two approaches have recently emerged for the visualization of air quality data. The first consists of the generation of a probability map of the areas around a receptor site that contribute to its poor air quality days, as characterized by high $PM_{2.5}$ and/or trace gas levels (the so-called Potential Source Contribution Function approach). This is the focus of our work in an upcoming publication [3]. The second approach was the focus of the present work and was based on grouping back trajectories with similar distances traveled or similar overall direction. It has been concluded that grouping back trajectories with similar distances traveled or similar overall direction is the best approach for the visualization of air quality data [4]. Cluster analysis, which uses physical distances between trajectories, has typically been used to group similar trajectories during the last two decades via algorithms like average-linkage clustering, Ward's method and k-means clustering [4]. These algorithms generate different classification results and their interpretation is often subjective. Consequently, there is no one best grouping algorithm [2,4–8].

Another grouping technique that has so far been overlooked for the classification of air mass back trajectories is neural network analysis. Neural networks have long been known as useful for analyses in synoptic climatology [9]. Since then,

* Corresponding author. Tel.: +1 416 978 1821; fax: +1 416 978 8605.
E-mail address: evansg@chem-eng.utoronto.ca (G.J. Evans).

0169-7439/$ - see front matter © 2006 Elsevier B.V. All rights reserved.
doi:10.1016/j.chemolab.2005.12.009

neural networks have found some use in general circulation models as they provide the tightest possible mapping of the complex, non-linear relationships between the atmosphere and the surface environment [10]. However, a study of transport patterns of air masses, a less complex problem, has not emerged.

The neural network approach differs from cluster analysis in that a desired degree of separation must be specified rather than a desired number of clusters. Secondly, the dot product used in neural net classification incorporates an angular component, relatable in this application to wind direction, rather than the geometric distance used in cluster analysis. Finally neural nets are designed to learn: when a novel trajectory is encountered, a neural net will create a new class with this trajectory as its sole member. This feature can be incorporated into some cluster analysis algorithms but it is not fundamental to this method. Hence sufficient differences existed to suggest that the methods might produce different insight.

Air masses arriving in Toronto have diverse histories ranging from clean, fast-moving Arctic air to polluted, nearly stagnant Ohio Valley air. In fact, Southern Ontario $PM_{2.5}$ concentrations have been reported to be 2 to 4 times higher under southerly or southwesterly flow conditions than under northerly flow conditions [11]. Thus, the ideal trajectory taxonomy would not group trajectories that pass through both northerly and southerly regions before arriving in Toronto with purely northerly or southerly trajectories. Grouping of air trajectories has been used to study the origins of ozone pollution in Toronto [12]. However, this approach has not previously been applied to particulate matter in the region.

For this reason, the main goal of this work was a comparison of the air pollution information provided by cluster analysis and an artificial neural network, Adaptive Resonance Theory (ART-2a) [13–15], for back trajectories ending in Toronto during a thirteen month sampling duration. The adaptation of cluster analysis and ART-2a to interpret atmospheric pollutant concentration is described. The inter-cluster variation of atmospheric species concentration was also explored, with special attention devoted to those trajectory groups that displayed abnormally large or small concentrations of atmospheric particulate matter. Some reasons for the dissimilarity of the classifications are also suggested.

2. Methodology

2.1. Sampling of airborne pollutants

Urban Toronto $PM_{2.5}$ mass and number concentration, SO_2 concentration and Nitrate $PM_{2.5}$ mass concentration were measured for each hour in the sampling duration by a tapered element oscillating microbalance (TEOM 1400A, Rupprecht & Pataschnick Co.), aerodynamic particle sizer (APS) (Model 3321, TSI Inc.), and a real-time nitrate analyzer (Series 8400N, Rupprecht & Pataschnick Co.), respectively. Note that the APS provided a total particle number concentration between 0.5 and 2.5 μm in this work.

2.2. Compilation of back trajectories

Five-day back trajectories at an altitude of 500 m in Toronto, Ontario (43.8° N and −79.0° W), were calculated between January 14th 2002 and February 5th 2003 using HYSPLIT. HYSPLIT was provided by the Air Resources Laboratory of the United States National Oceanic and Atmospheric Administration [16]. Each back trajectory contained endpoints describing the hourly location of an air mass in latitude and longitude coordinates. Hence, every 5-day back trajectory had 120 endpoints (5×24), and 2880 endpoints (5×24×24) defined a single day. In this work, 10,100 back trajectories (24 per day over 421 days) were assigned to clusters and classes by cluster analysis and neural network analysis, respectively.

2.3. Cluster analysis of back trajectories

The application of cluster analysis to back trajectory taxonomy has been documented in detail by Cape et al. [4] and Dorling et al. [8]. In particular, Dorling's method, which was used in this work, has been noted to discriminate distinct flow patterns and large scale circulation features effectively [17]. Briefly, the distances between Toronto and each of the 120 endpoints of a trajectory were calculated as kilometers north and east of Toronto, assuming a spherical earth. As suggested by Cape et al. [4], trajectories were then reduced to 11 endpoints, representing the location of the trajectory at 12-h intervals starting from Toronto. Next, average-linkage clustering using the Euclidean distances between trajectory endpoints was performed on these reduced trajectories [4,8].

Finally, the optimal number of clusters was deduced by calculating the root mean square deviation between the average trajectory of a cluster and its member trajectories. A cumulative root mean square deviation (RMSD) was determined for all the clusters, and recalculated as clusters with the most similar average trajectories were combined. Fig. 1 illustrates the percent change in the total RMSD as the number of clusters decreased from an initial 25. Values immediately preceding local minima represent the joining of dissimilar clusters [8], thus permitting a logical, if somewhat subjective, choice for the optimal number

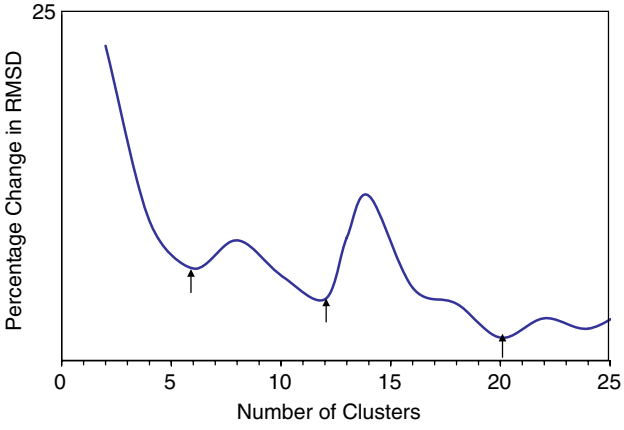

Fig. 1. Choosing an optimal number of clusters via changes in RMSD.

of clusters [4]. While 6, 12 and 20 cluster solutions were favourable, the 12 cluster solution was chosen because it represented a compromise between significant transport pattern variation and ease of analysis.

2.4. Neural network analysis of back trajectories

The latitude and longitude 12-hourly endpoints of all the 5-day back trajectories (ending 500 m above Toronto) were first organized into latitude and longitude matrices. Note that the same data was used in the cluster analysis procedure described in Section 2.3. Each row in both matrices represented an individual back trajectory, while each column represented the location of a trajectory for each hour prior to arrival in Toronto. Thus, both matrices had 10,100 rows and 11 columns. Every column was standardized to a mean of zero and standard deviation of unity across its 10,100 back trajectories to enhance the classification ability of the neural network ART-2a. Standardized back trajectories were subsequently normalized to yield unit vectors, a necessary step for classification by ART-2a [13–15]. While the necessity of normalization becomes evident in the next paragraph, the standardization of the data was necessary to reduce computational difficulty of the classification.

Typically, the centroids of each created class were stored as vectors called "weights" in a weights matrix. In this case, each trajectory was represented by two variables, and thus the centroids of each class were stored in latitude weights and longitude weights matrices. Furthermore, the dot-product of a latitude weight vector and a trajectory latitude vector, as well as that of the corresponding longitude vectors, described the extent of similarity between each trajectory and a created class. The smaller of the two dot-products needed to be larger than a user-defined similarity criterion (termed the vigilance factor) for the given back trajectory to be classified as a resonant trajectory.

$$\text{If} \begin{bmatrix} x_1 \\ \vdots \\ x_{12D} \end{bmatrix} \cdot \begin{bmatrix} u_1 \\ \vdots \\ u_{12D} \end{bmatrix} > p, \quad \text{AND} \begin{bmatrix} y_1 \\ \vdots \\ y_{12D} \end{bmatrix} \cdot \begin{bmatrix} w_1 \\ \vdots \\ w_{12D} \end{bmatrix} > p, \quad \text{RESONANCE}$$

$$\text{Else,} \qquad \text{NOVELTY}$$

where x_i and y_i are latitude and longitude trajectory vectors, u_i and w_i are latitude and longitude weight vectors of a given class, respectively, and ρ denotes the vigilance factor. Note that a novel class was only created after the dot products of a trajectory vector with all the existing class weight vectors had been evaluated and not found to satisfy the above criterion. Typically, a trajectory is chosen at random to be the weight vector for the first class, and other trajectories are compared to this. As new classes are created, a small percentage (termed the learning rate and set to 6% in our work) of the trajectories newly added into a given class is added to the individual weight vectors to better reflect the instantaneous class population. The weight vectors at the end of the first iteration were the input weights for the beginning of the second iteration. Trajectories were again sampled randomly and reclassified. In this manner, ten iterations, called epochs, were run. We had previously determined that using ten epochs and a 6% learning rate reduces misclassifications (defined as trajectories that are continually classified into different classes in each iteration) to less than 5%. If a trajectory was resonant with more than one class, it was added to the class with whose weight vectors it had the largest dot product.

In this work, a solution containing 12 ART-2a classes was generated to facilitate comparison with the 12 cluster solution. This represented a choice of 0.02 for the vigilance factor. Note that increasing the vigilance could help identify exceptional trajectory patterns. While this increases the overall number of classes, it is still a great advantage of using ART-2a. Additionally, classification of hourly latitude and longitude endpoints, and thus a $10{,}100 \times 121$ sized matrix, produced results very similar to those from the classification of 12-hourly endpoints. For the sake of simplicity, however, only the results of the ART-2a and cluster analysis classifications of 12-hourly endpoints are presented in this work.

Finally, the precision of both solutions was determined. The angle between a trajectory endpoint and its corresponding class/cluster average trajectory endpoint, with Toronto as the vertex, was calculated. The median angular deviation of the members of a class/cluster from its average trajectory (based on several thousand angular deviations) was chosen to represent the similarity of trajectories grouped together and thus the precision of the trajectory assignments generated.

3. Results and discussion

3.1. Comparison of cluster analysis and ART trajectory classifications

Since this was the first application of ART-2a to back trajectory analysis, a comparison between the ART and cluster analysis solutions follows. Due to the different similarity criteria, each ART class was composed of trajectories that were placed in different clusters. Fig. 2 illustrates an example to explain the reasons behind the different trajectory assignments and to highlight some associated implications.

Trajectories 1 and 3 were assigned to one ART class (class 7), while trajectories 1 and 2 were assigned to the same cluster (cluster 8). Note that while trajectories 1 and 2 traveled similar distances, trajectories 1 and 3 were alike in their overall shape. Hence, cluster analysis did not appear to consider the overall shape of trajectories as important as the inter-trajectory distances. The reasons behind this difference are twofold: firstly, while the ART input data was standardized and normalized, the cluster analysis input data was not, by necessity; secondly, the ART-2a similarity criterion was bounded between -1 and 1, whereas that of cluster analysis was not. This resulted in two alternate but equally valid classifications, one based on the inter-trajectory distances, the other on similarity of overall shape. While inter-trajectory distances must be considered to prevent the grouping of fast- and slow-moving trajectories and thus the obscuring of stagnation effects, the overall direction must also be borne in

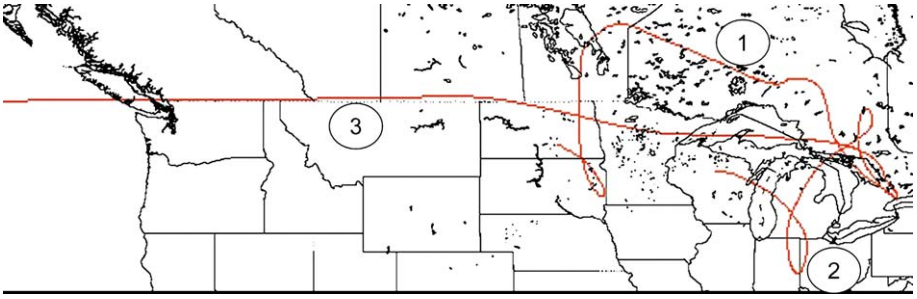

Fig. 2. Demonstrating the classification schemes by three trajectories grouped differently by cluster analysis and ART-2a.

mind to prevent the grouping of trajectories passing through different geographic areas and thus the misidentification of possible source regions.

Finally, the precision of both solutions was determined as described in Section 2.4. Fig. 3 shows that while the median angles for the 12 clusters are less scattered than the 12 corresponding ART-2a angles, one of these angles (cluster 2) is quite large. Thus, a risk of data misinterpretation existed, as is described in the following discussion.

Overall, however, both techniques can be seen to provide similarly precise solutions. Note that those classes/clusters that exhibited median angles beyond the interquartile range (shown as larger points on Fig. 3) are referred to as "blurred" in the following discussion.

3.2. Cluster analysis classification results

Fig. 4 illustrates the average trajectories, also referred to as transport patterns, of the twelve clusters created by cluster analysis. The "blurred" clusters 2, 4, 8, 10, 11 and 12 accounted for 63% of the trajectories. In addition, clusters 2, 8, and 12 were short transport patterns indicative of slow-moving air masses. Consequently, assuming the presence of upwind emission sources and low mixing heights, elevated airborne pollutant concentrations were anticipated in Toronto for these transport patterns.

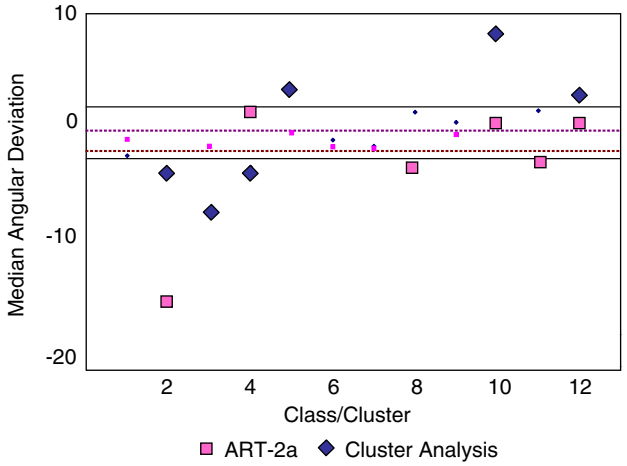

Fig. 3. The precision of the cluster analysis and ART-2a solutions. Each point represents the median value of the angles between trajectory endpoints and their corresponding cluster/class average trajectory endpoints. The dotted and solid horizontal lines represent the interquartile ranges of the 12 median angles for cluster analysis and ART-2a, respectively.

3.3. Application to air pollution data

The clusters were ordered to provide an approximate north-to-south, anti-clockwise variation. Clusters containing less than 50 trajectories were not displayed. Fig. 5A and B illustrate the variation of the median concentration of atmospheric particulate matter in Toronto with transport pattern.

In general, all three pollutant measurements exhibited smaller concentrations for northerly transport patterns, and larger concentrations for those passing through the Midwestern United States. This observation may be attributed to the large numbers of power plants and industries located south and southwest of Toronto, consistent with previous work [11]. These regions have three Canadian power plants, Lakeview (Mississauga, Ontario), Lambton (Sarnia, Ontario) and Nanticoke (Nanticoke, Ontario), and the many U.S. power-generating stations in the Ohio Valley. However, clusters 2, 8, 10, 11 and 12 displayed unusual behaviour in this general trend. Note that clusters 10 and 11 were small clusters containing about 1% of the trajectories each. Detailed explanations for these observations follow.

The largest $PM_{2.5}$ mass concentrations were found in clusters 2, 8, 11, and 12. Some of the trajectories assigned to cluster 2 were northerly ones that entered the Ohio Valley before doubling back to Toronto. Meanwhile, cluster 8 displayed northwesterly trajectories that passed both north and south of the Great Lakes, resulting in the "blurring" of this cluster. Its elevated $PM_{2.5}$ mass concentration was suggested to originate from agricultural areas in Michigan and Southern Ontario and to be enhanced due to its slow-moving nature causing the accumulation of $PM_{2.5}$. The similar but smaller $PM_{2.5}$ mass concentrations of adjacent clusters support this hypothesis. Clusters 11 and 12 displayed the largest $PM_{2.5}$ mass concentrations, which were expected due to their transport through the industrialized Ohio Valley. Finally, the Toronto $PM_{2.5}$ mass concentration appeared to be dependent more on the transport pattern than the season the pattern appeared most frequently in. For example, clusters 4 and 11 exhibit very different $PM_{2.5}$ mass concentrations even though they both appeared primarily in the winter and spring seasons.

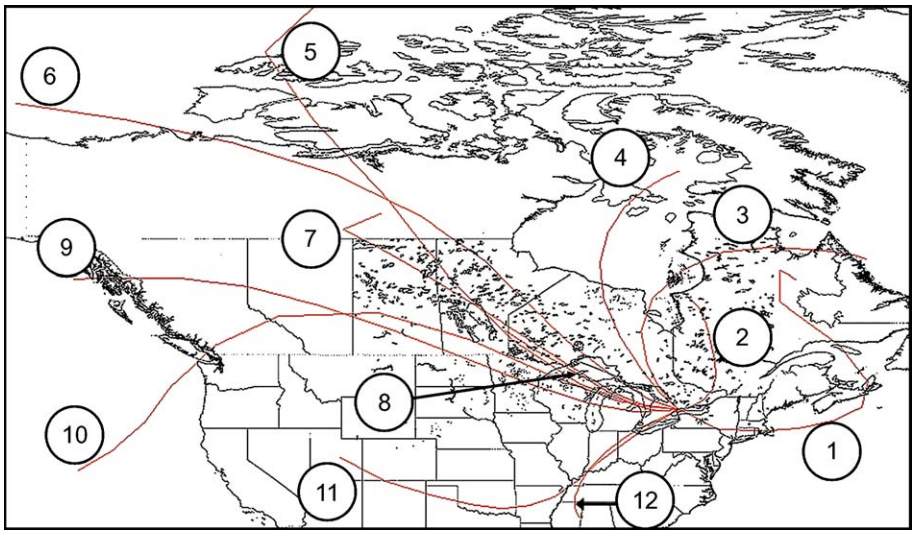

Fig. 4. Transport patterns created by cluster analysis.

Clusters 2, 8, 11, and 12 also displayed elevated $PM_{2.5}$ number concentrations. The explanation suggested for the $PM_{2.5}$ mass concentrations of these clusters was applicable once again. Interestingly, the median of the ratios of each cluster's $PM_{2.5}$ number and mass concentrations was approximately 1.1. While the absolute value of the ratio held little meaning, large deviations from the median ratio value highlighted the relative size of particles in each cluster. Clusters 11 and 12 displayed ratios of 3.2 and 2.3, respectively, indicating the presence of finer particles in Toronto air under southerly and southwesterly flow conditions than under north and northwesterly flow conditions. Hence, the secondary formation of $PM_{2.5}$ leading to finer particles was suggested to be relatively larger for southerly regions than northerly regions. This is supported by the number / mass ratio of cluster 6, a very long transport pattern that contained the coarsest $PM_{2.5}$ observed. This is understandable since industrial sources were present in regions south of Toronto. Similar to the $PM_{2.5}$ mass concentration, the $PM_{2.5}$ number concentration appeared to be dependent more on the transport pattern than the season the pattern appeared most frequently in.

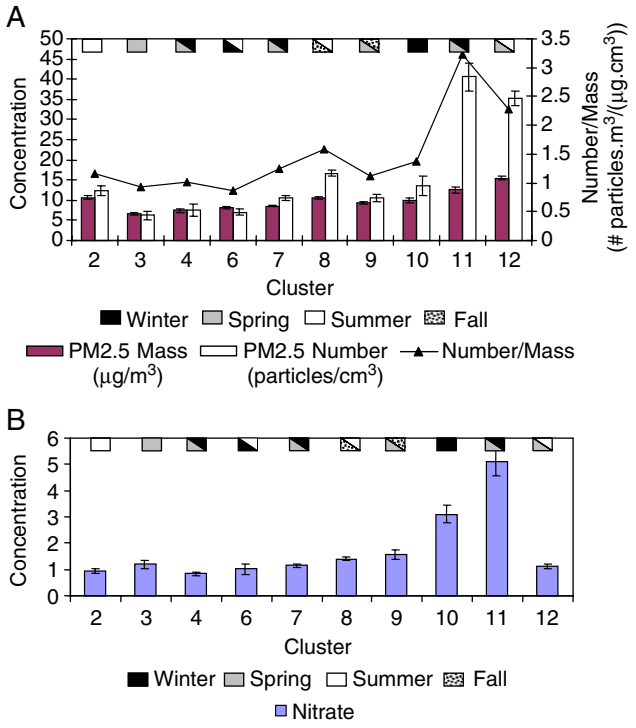

Fig. 5. Effect of changing cluster analysis transport patterns on Toronto (A) $PM_{2.5}$ mass and number median concentrations, and (B) $PM_{2.5}$ nitrate median concentration. All median concentrations are in µg/m^3 or #/cm^3. The standard errors on the median values and the season(s) during which over 25% of trajectories in a given cluster were observed are also noted.

Clusters 10 and 11 exhibited elevated $PM_{2.5}$ nitrate mass concentration. These were primarily winter-based clusters (cluster 11 also appeared during the spring) and their elevated nitrate concentrations were understandable given the bias of nitrate towards cooler seasons [18]. Furthermore, agricultural activity is known to be an important source of nitrate precursors like NH_3 [19], although cars have recently been proposed to be a substantial source of NH_3 in urban environments [20]. In addition, less oxidation of SO_2 to sulphate occurs during winter, leaving more NH_3 for gaseous nitric acid to react with [19]. The condensation of ammonium nitrate from biogenic activities in Southern Ontario and Michigan during colder temperatures onto particles originating upwind is proposed. This hypothesis is supported by the small nitrate content of cluster 12, a primarily summer based group. Note that clusters 4, 6, and 7, which are also winter-based clusters, did not exhibit elevated nitrate concentrations stressing the importance of transport through Southern Ontario and Michigan for the appearance of $PM_{2.5}$ nitrate in Toronto. If the ammonium nitrate observed in Toronto was only produced from local NO_x and NH_3 emissions, then one would not expect the $PM_{2.5}$ nitrate concentration to show a trajectory-related dependence. Conversely, the trajectory independent background concentration of about 1 µg/m^3 might be taken as a measure of the locally produced $PM_{2.5}$ nitrate

concentration. This also suggests that much of the NH_3 and NO_x precursors of ammonium nitrate produced within Toronto go on to produce nitrate PM downwind.

3.4. ART classification results

Fig. 6 illustrates the twelve, five-day transport patterns, also called classes, created by ART-2a. The "blurred" classes 2, 3, 4, 5, 10, and 12 accounted for 47% of the trajectories (cf. 63% in the cluster analysis case). This suggested a somewhat more effective separation of trajectories into distinct transport patterns by ART-2a than by cluster analysis. In addition, classes, 9, 11, and 12 displayed shorter transport patterns than others, indicative of a longer residence time. Since they also traveled through the Midwestern United States, larger airborne pollutant concentrations in Toronto were anticipated for these transport patterns.

3.5. Application to air pollution data

The classes were ordered to provide an approximate north-to-south, anti-clockwise variation. Fig. 7A and B illustrates the variation of the median concentration of each atmospheric pollutant measurement with transport pattern. Similar to Fig. 5A, the median $PM_{2.5}$ mass and number concentrations were generally largest under southerly and southwesterly flow conditions. Furthermore, the northernmost flow pattern of Class 1 is not as polluted as that of the northernmost cluster 2, demonstrating the removal of the northerly trajectories that

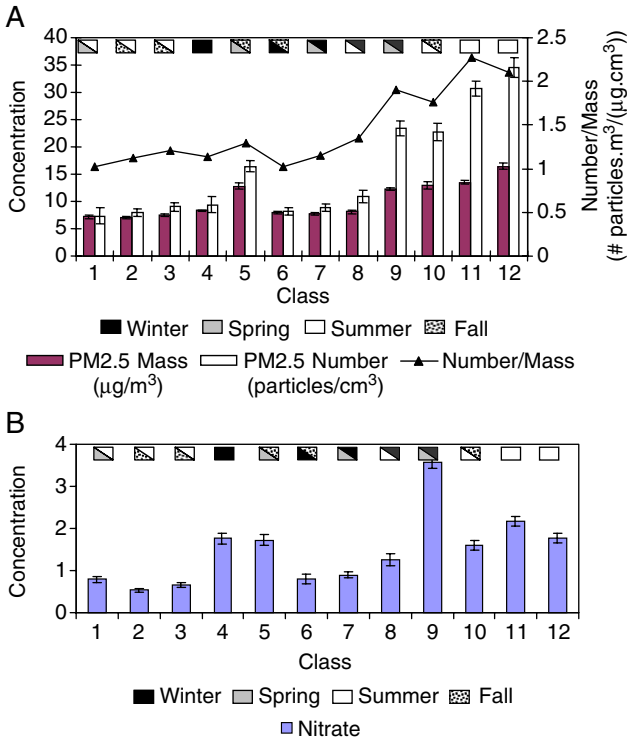

Fig. 7. Effect of changing ART-2a transport patterns on Toronto (A) $PM_{2.5}$ mass and number median concentrations, and (B) $PM_{2.5}$ nitrate median concentration. All median concentrations are in $\mu g/m^3$ or $\#/cm^3$. The standard errors on the median values and the season(s) during which over 25% of trajectories in a given class were observed are also noted.

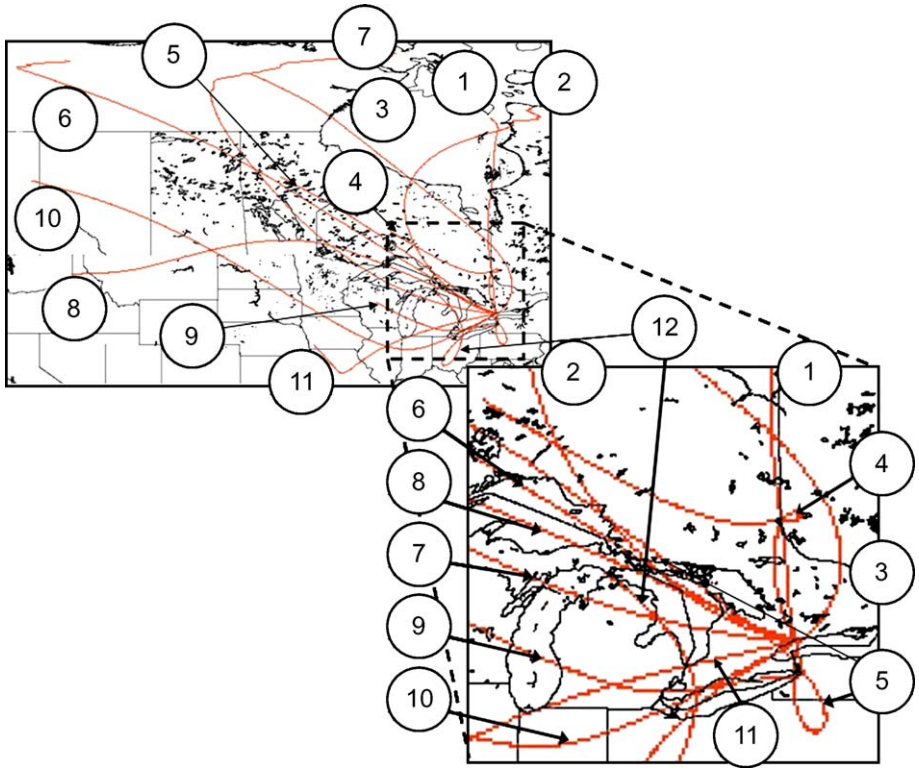

Fig. 6. Transport patterns created by ART-2a.

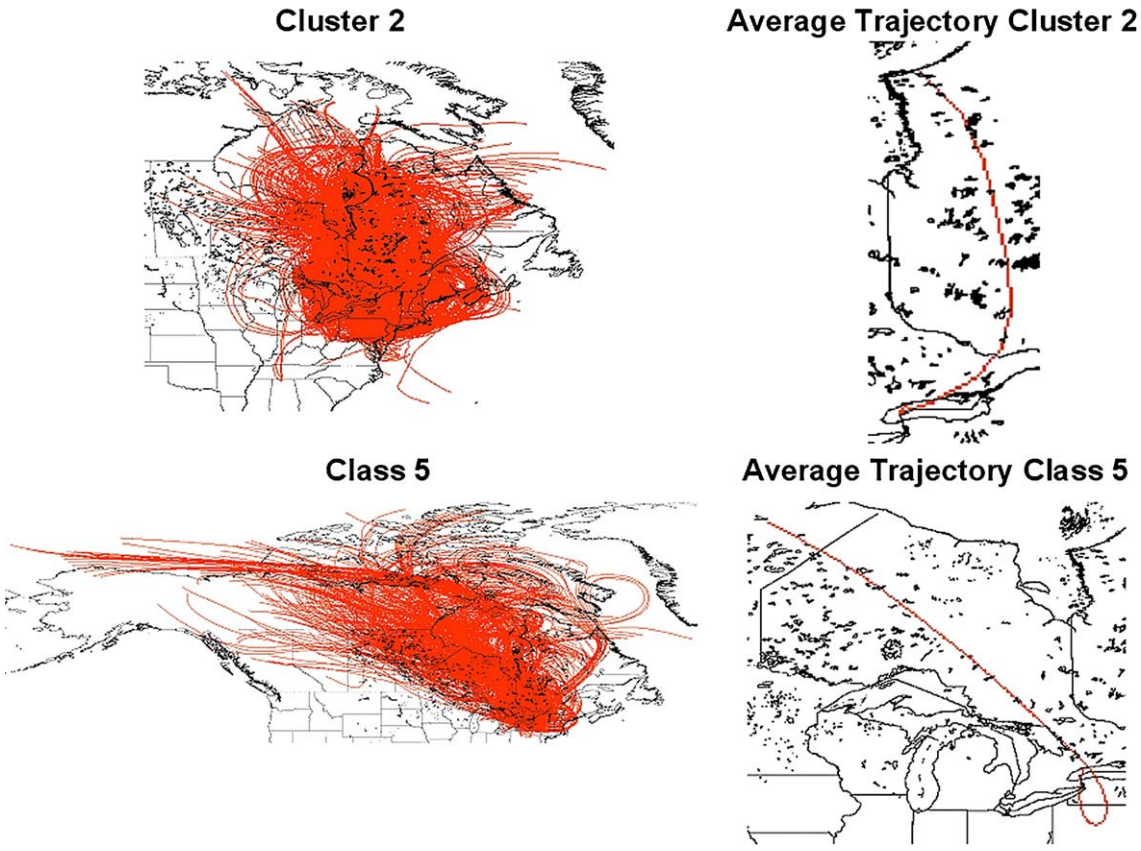

Fig. 8. Depiction of the differences between the northern-most cluster and class produced through cluster analysis and ART-2a.

traveled south before doubling back to Toronto. ART-2a assigned these trajectories to class 5, as seen in Fig. 8. However, the $PM_{2.5}$ nitrate concentrations follow somewhat different trends, as evidenced by Fig. 7B, which have been explained in the following discussion. The impact of stagnant conditions on downwind pollution levels was evident for classes 9, 11, and 12, and similar to the behaviour of clusters 8, 11 and 12, respectively. As with the cluster analysis results, the combination of stagnant conditions and the presence of emission sources in Southern Ontario pollution and the Ohio Valley is suggested to account for the ART-2a results.

The largest $PM_{2.5}$ mass concentrations were found in classes 5, 9, 10, 11, and 12. The large concentration associated with class 5, which goes against the general trend of cleaner northerly air, is due to the passage of its member trajectories through areas south of Toronto, western New York in this case. Note that this concentration is comparable to those associated with transport patterns traveling through the Ohio Valley, classes 9 through 12. Note also the lack of seasonal effects on the $PM_{2.5}$ mass concentration: clearly, transport through regions south and southwest of Toronto in any season results in higher mass levels as compared to passage through north and northwesterly regions. An argument similar to that for $PM_{2.5}$ nitrate shown in the previous section suggests that a trajectory independent $PM_{2.5}$ mass concentration of 10 $\mu g/m^3$ is likely emitted and/or produced locally. This agrees closely with previous studies [19].

Classes 5, and 9 through 12, also emerged dominant for the $PM_{2.5}$ number concentrations. The explanation suggested for the $PM_{2.5}$ mass concentrations of these classes was applicable once again. While the median of the ratios of each cluster's $PM_{2.5}$ number and mass concentrations was approximately 1.1, the corresponding ART-2a value was 1.25. The largest deviations were evident for classes 9 through 12, once again demonstrating the finer nature of particles in Toronto under southerly and southwesterly flow conditions. Similar to the $PM_{2.5}$ mass concentration, no appreciable seasonal effects were observed on the variation of Toronto $PM_{2.5}$ number concentration with change in transport pattern.

The $PM_{2.5}$ nitrate mass concentrations of classes 4, 5, and 9 were distinctly elevated. Note that the winter-based class 9 passed through Southern Ontario and Michigan, and as with clusters 10 and 11, the condensation of ammonium nitrate from biogenic activities onto particles originating upwind during colder temperatures is proposed. This hypothesis is supported by the back trajectories in Class 9 occurring mainly during the winter season, and by the smaller nitrate levels of Classes 11 and 12, which favoured warmer seasons. Similarly, although classes 4 and 5 displayed more northerly transport patterns, they also traveled through Southern Ontario and thus displayed comparable nitrate content.

4. Conclusions

In this paper, back trajectories of air masses arriving in Toronto were classified into distinct transport patterns by cluster analysis and a neural network (ART-2a). The application of bulk data to the classification of air mass back trajectories by cluster analysis and a neural network (ART-2a) demonstrated that both techniques provide similar conclusions as to the location of emission sources and the level of pollution associated with a given air transport pattern. Both techniques illustrated the cleaner nature of northerly and northwesterly transport patterns in comparison to southerly and southwesterly ones, as well as the effect of near stagnant air masses, despite the different similarity criteria used by the two classification techniques. In addition, ART-2a resolved a somewhat larger percentage of trajectories than cluster analysis into groups with clearly identifiable transport patterns, and compared favourably with it with respect to the precision of classification.

Acknowledgements

The authors thank the Canada Foundation for Innovation, Ontario Research and Development Challenge Fund, Natural Sciences and Engineering Research Council (NSERC), Environment Canada, and the Ontario Ministry of the Environment, for funding to construct and operate the University of Toronto Facility for Aerosol Characterization. The authors are also grateful to Environment Canada for the TEOM results and the loan of the nitrate analyzer.

References

[1] Ontario Medical Association (Ed.), The illness costs of air pollution—findings report, http://www.oma.org/phealth/icap.htm (2000) (Accessed August 2003).
[2] A. Stohl, Atmos. Environ. 32 (1998) 947–966.
[3] S. Owega, G.J. Evans, B. Khan, R.E Jervis, M. Fila, Ecological modelling (submitted for publication).
[4] J.N. Cape, J. Methven, L.E. Hudson, Atmos. Environ. 34 (2000) 3651–3663.
[5] E. Brankov, S.T. Rao, P.S. Porter, Atmos. Environ. 32 (1998) 1525–1534.
[6] L.A. Moy, R.R. Dickerson, W.F. Ryan, Atmos. Environ. 28 (1994) 2789–2800.
[7] M.E. Fernau, P.J. Samson, J. Appl. Meteorol. 29 (1990) 735–761.
[8] S.R. Dorling, T.D. Davies, C.E. Pierce, Atmos. Environ. 26A (1992) 2575–2581.
[9] B. Yarnal, A.C. Comrie, B. Frakes, D.P. Brown, Int. J. Climatol. 21 (2001) 1923–1950.
[10] E. Zorita, H. von Storch, J. Climate 12 (1999) 2474–2489.
[11] J.R. Brook, C.D. Lillyman, M.F. Shepherd, A. Mamedov, J. Air Waste Manage. 52 (2002) 855–866.
[12] E. Brankov, R.F. Henry, K.L. Civerolo, W. Hao, S.T. Rao, P.K. Misra, R. Bloxam, N. Reid, Environ. Pollut. 123 (2003) 403–411.
[13] X.H. Song, P.K. Hopke, D.P. Fergensen, K.A. Prather, Anal. Chem. 71 (1999) 860–865.
[14] D.J. Phares, K.P. Rhoads, A.S. Wexler, D.B. Kane, M.V. Johnston, Anal. Chem. 73 (2001) 2338–2344.
[15] O. Malpica, MASc Dissertation, University of Toronto, 2002.
[16] R.R., Draxler, 1992. NOAA Tech. Memo. ERL ARL-195, 26 pp. and Appendices.
[17] A. Stohl, H. Scheifinger, Meteorol. Z. 6 (1994) 333–336.
[18] P.A. Makar, H.A. Wiebe, R.M. Staebler, S.M. Li, K. Anlauf, J. Geophys. Res. 103 (1998) 13095–13110.
[19] J. Tsai, MASc Dissertation, University of Toronto, 2002.
[20] C. Perrino, M. Catrambone, A. Di Menno Di Bucchianico, I. Allegrini, Atmos. Environ. 36 (2002) 5385–5394.